Available online at www.sciencedirect.com
ScienceDirect
Trans. Nonferrous Met. Soc. China 22(2012) 1018−1027
Transactions of Nonferrous Metals Society of China
www.tnmsc.cn

Comparative study on corrosion behavior of as-cast and extruded Mg−5Y−7Gd−1Nd−0.5Zr alloy in 5% NaCl aqueous solution

ZHANG Xin[1,2,3], ZHANG Kui[1], LI Xing-gang[1], DENG Xia[1],
LI Hong-wei[2,3], ZHANG Bao-dong[2,3], WANG Chang-shun[2,3]

1. State Key Laboratory for Fabrication and Processing of Nonferrous Metals, Beijing General Research Institute for Non-ferrous Metals, Beijing 100088, China;
2. Institute of Technology, Beijing North Vehicle Group Corporation, Beijing 100072, China;
3. Beijing Engineering Research Center for Advanced Manufacturing and Evaluation of Special Vehicle Parts, Beijing 100072, China

Received 6 April 2011; accepted 30 August 2011

Abstract: The corrosion behaviours of Mg−5Y−7Gd−1Nd−0.5Zr magnesium alloys prepared by as-casting and extrusion were investigated in 5% NaCl aqueous solution by immersion and electrochemical tests. The microstructure indicates the mean grain size of 15 μm for the extruded and 100 μm for the as-cast Mg−5Y−7Gd−1Nd−0.5Zr magnesium alloys. The corrosion morphology of as-cast sample shows pitting corrosion and little filiform corrosion, but that of the extruded sample shows pitting corrosion at the initial stage. The corrosion rate of extruded sample is higher than that of as-cast Mg−5Y−7Gd−1Nd−0.5Zr alloy according to the immersion test. The second phases containing RE acting as cathodes improve the corrosion properties. The corrosion potentials of as-cast and extruded Mg−5Y−7Gd−1Nd−0.5Zr alloys are −1.658 V and −1.591 V, respectively. The origins of the distinctive corrosion behavior of as-cast and extruded Mg−5Y−7Gd−1Nd−0.5Zr Mg alloys were discussed.
Key words: Mg−5Y−7Gd−1Nd−0.5Zr magnesium alloy; corrosion morphology; polarization curve

1 Introduction

Mg and Mg alloys are regarded as green and promising structural metallic materials in the 21st century, and have great potentials in industrial applications, especially in aviation and transportation fields [1−3]. However, their applications are still limited due to several undesirable properties, such as relative low strength, low ductility, especially poor corrosion resistance. The corrosion resistance of the Mg-based alloys is generally inadequate due to the low standard electrochemical potential of −2.37 V compared with the standard hydrogen electrode (SHE) [4] and this limits the range of applications of Mg and its alloys. Grain refinement has been proved to be favorable to improving both mechanical property and corrosion resistance of Mg and its alloys, and several methods developed for refining the grain of Mg alloys have been divided into the following groups: 1) cold or warm rolling plus heat treatment involving recrystallization, 2) hot extrusion at a high extruded ratio, 3) hot working on Mg alloys, 4) severe plastic deformation processes such as torsion straining [5], reciprocal extrusion [6], and equal channel angular extrusion (ECAE) [7]. The process has been widely investigated in the last decades via extrusion. The extrusion has shown to be effective and commercial in refining grains in various Mg alloys with improved ductility, strength, and plasticity, especially corrosion resistance. Herein, the extrusion deserves attention as one of the most attractive grain-refining methods to improve the corrosion resistance [8−10]. BEN-HAROUSH et al [11] and BEN-HAMU et al [12] reported that the corrosion resistance of AZ80 and AZ31 alloy was decreased after extrusion.

Magnesium alloys containing heavy rare earth elements are becoming more and more attractive due to their high strength and ductility. They have large potential applications as light structural materials for the aerospace and racing automotive industries. It is well

Foundation item: Project (2011BAE22B01) supported by the National Key Technology R&D Program of China
Corresponding author: ZHANG Xin; Tel: +86-10-83807347; E-mail: bjzx201@yahoo.com.cn
DOI: 10.1016/S1003-6326(11)61278-8

known that the addition of rare earth (RE) elements is an effective way to improve the mechanical properties of magnesium. Corrosion behavior of magnesium alloy with RE element has been investigated. The Mg−RE−Zr magnesium alloy system, which usually contains Y, Nd, Gd and some other rare-earth elements, is the most successful magnesium alloys in this category at present, such as WE43, WE54, Mg−5Y−7Gd−1Nd−0.5Zr. In the Mg−RE−Zr magnesium alloy system, Mg−5Y−7Gd−1Nd−0.5Zr magnesium alloy was invented by LI et al [13], which is used widely in the aeronautics and astronautics. The excellent performance of Mg−5Y−7Gd−1Nd−0.5Zr alloy has been achieved in industrialized tests and meets the demands of industrial productions which need high performance magnesium alloy.

As for the corrosion behaviour of the Mg−RE−Zr magnesium alloy system prepared by as-casting and extrusion, there are several reports [14−16], and they present better anti-corrosion properties than Mg−Al, Mg−Mn and other magnesium alloy systems. However, the content of RE has a significant effect on the mechanical property and corrosion behavior. QUACH et al [17] and ZHANG et al [18] produced magnesium metals containing rare earth elements. The corrosion resistance was improved greatly by a small content of RE, whereas the excess addition of RE deteriorated the corrosion resistance.

In the present study, the basal corrosion behavior of Mg−5Y−7Gd−1Nd−0.5Zr magnesium alloys in 5% (mass fraction) NaCl aqueous solution was investigated at room temperature. The objectives of this study were to investigate the corrosion and electrochemical behaviors of the as-cast Mg−5Y−7Gd−1Nd−0.5Zr magnesium alloy in 5% NaCl aqueous solution and correlate them with the changes of the corrosion morphologies, corrosion rate and the electrochemical behaviors caused by extrusion.

2 Experimental

2.1 Test materials

Yttrium, neodymium, gadolinium, and Mg−30Zr master alloys as the raw materials were used to prepare the Mg−5Y−7Gd−1Nd−0.5Zr magnesium alloys. All the alloys were melted in a mild steel crucible with the protection of homemade flux. When the fused mass temperature reached 1023 K, the yttrium, neodymium, and gadolinium were added into the crucible, and then the temperature was raised to 1123 K and kept for 20 min. Finally, the Mg−30Zr master alloys were put into the molten metals and stirred for 5 min, and then poured into a steel mold with a diameter of 98 mm [14]. Mg−5Y−7Gd−1Nd−0.5Zr magnesium alloys in this study were prepared by ingot casting process according to industrial casting norm specimens, which have dimensions of 10 mm × 10 mm × 10 mm, for all the experiments. The actual compositions of the Mg−5Y−7Gd−1Nd−0.5Zr magnesium alloys studied were determined by inductively coupled plasma-atomic emission spectrometry (ICP-AES), and the results of the alloy are presented in Table 1.

Table 1 Nominal composition of MG−5Y−7GD−1ND−0.5ZR (mass fraction, %)

Y	Gd	Nd	Zr	Mg
4.53	7.04	1.29	0.49	Bal.

The materials used for extrusion process were cut from as-cast Mg−5Y−7Gd−1Nd−0.5Zr magnesium ingots. The schematic illustration of the extruded process is shown in Fig. 1. The diameters of extrusion billet and extrusion specimen were 90 cm and 50 cm, respectively, with a plunger speed of 0.5 mm/s at 573 K. Graphite was used as lubricant to reduce the friction coefficient between the billet and the die inner wall. The experiments presented that extruded samples without any micro-cracks could be fabricated at the optimal temperature (573 K) and the above pressing parameters.

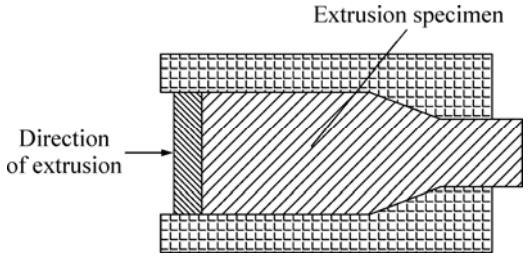

Fig. 1 Schematic illustration of extrusion process

The structure of the samples was investigated by grazing incidence X-ray diffraction. X-ray diffraction patterns were recorded with an X-ray diffractometer, using Cu $K_{\alpha 1}$ (λ=0.154056 nm) radiation at a constant incidence angle of 1° to the specimen surface in a θ–2θ geometry. Crystalline phases were identified using the JCPDS database cards.

2.2 Immersion tests

For metallographic characterization, samples were wet ground through successive grade of silicon carbide abrasive papers from P120 to P2000 followed by diamond finishing to 0.1 μm, followed by rinsing with isopropyl alcohol in an ultrasonic bath and drying in warm air. In all cases, the tests were performed in duplicate to guarantee the reliability of the results. Cleaning the corrosion products of the specimens in the experiment was done by dipping in a 400 mL aqueous solution of 10% CrO_3 (mass fraction)+1% $AgNO_3$ under

boiling condition, then products were dried by hot air flow and reweighed to obtain the mass loss.

JSM−6510A analytical scanning electron microscope (SEM) equipped with an energy dispersive X-ray spectrometer (EDS) was used to observe the corrosion morphologies and analyze the elements. Lycar MZ6 was used to observe the microstructure. The specimens for SEM were revealed with 4% nitric acid in alcohol.

2.3 Electrochemical measurements

The open circuit potential and the polarization curves were obtained in 5% NaCl solution saturated with $Mg(OH)_2$ using a Potentioatat/Galvanostat Model 273A. A classical three-electrode cell was used with platinum as counter electrode, saturated calomel electrode SCE (0.242 V vs SHE) as reference electrode, and the sample as working electrode. The samples were mounted using epoxy resin and only left an exposed area of 1 cm^2. The lasting time of the open circuit potential test was 9 h. The measurements began from the cathodic side at a constant voltage scan rate of 0.5 mV/s after the initial retard of 300 s.

3 Results and discussion

3.1 Microstructures of samples

Figure 2 shows the microstructures of the as-cast and extruded Mg−5Y−7Gd−1Nd−0.5Zr magnesium alloys. The as-cast sample was characterized by an average grain size of 100 μm (Fig. 2(a)). The microstructure after conventional extrusion at 573 K is shown in Fig. 2(b). Although many grains are already significantly refined after the extrusion process, the grain structure is not homogeneous, with very fine grains of 15 μm as well as coarse grains greater than 30 μm.

Figure 3 indicates the results of X-ray diffraction analysis of Mg−5Y−7Gd−1Nd−0.5Zr Mg alloys prepared by casting (Fig. 3(a)) and extrusion (Fig. 3(a)), respectively. The phase composition of the alloy almost is not changed, and still consists of matrix phase α-Mg and the eutectic phases of $Mg_{24}Y_5$, $Mg_{41}Nd_5$, and Mg_5Gd.

3.2 Mass loss measurements

With respect to the determination of corrosion rate, the most accurate and precise method is probably mass loss measurement [19,20]. The corrosion rate variation with the immersion time during the immersion testing, average corrosion rates of as-cast and extruded Mg−5Y−7Gd−1Nd−0.5Zr Mg alloys are shown in Table 2. Two obvious trends could be deduced from the curves, the corrosion rate of extruded sample is higher than that of as-cast sample in 5% NaCl aqueous solution; the

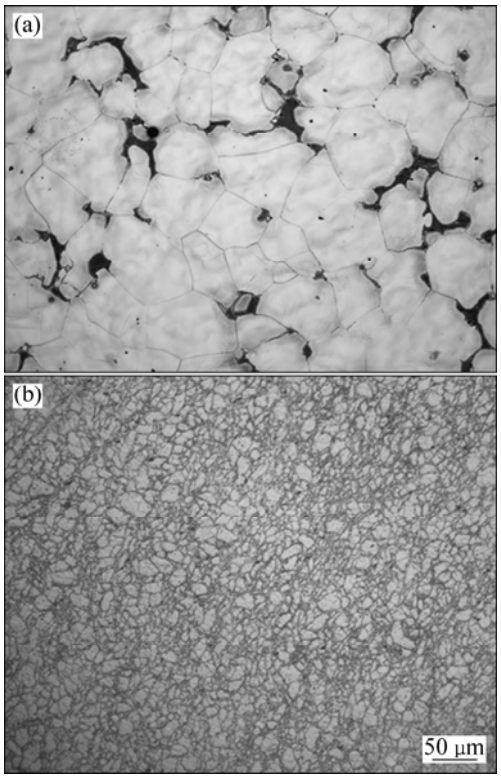

Fig. 2 Microstructures of as-cast (a) and extruded (b) Mg−5Y−7Gd−1Nd−0.5Zr Mg alloy

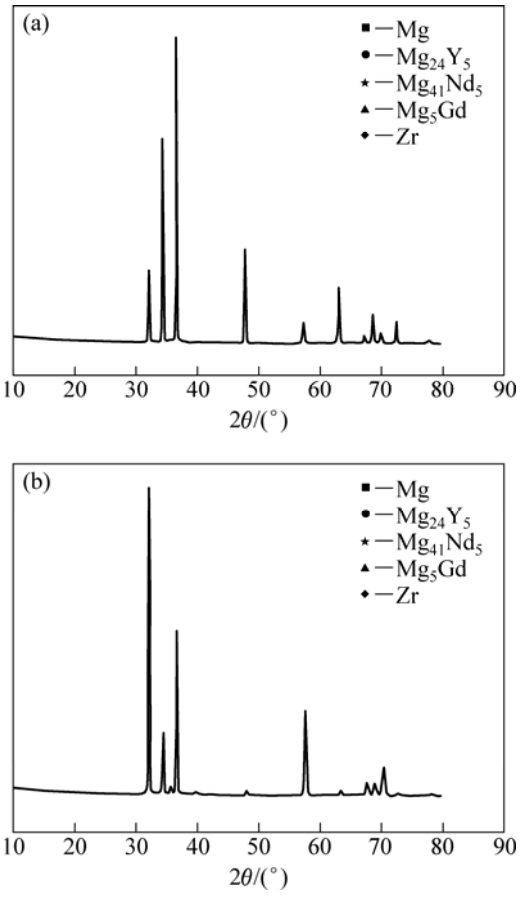

Fig. 3 XRD patterns of as-cast (a) and extruded (b) samples

corrosion rates of the two samples decrease with increasing immersion time because the stacked corrosion products have little protective effect, and the decrease in corrosion rate may relate to the increase of pH value of the solution caused by the dissolution of $Mg(OH)_2$ [21,22].

Table 2 Average corrosion rates of as-cast and extruded Mg−5Y−7Gd−1Nd−0.5Zr Mg alloys

Alloy	Corrosion rate/(g·m^{-2}·h^{-1})	
	2 h	24 h
As-cast alloy	0.303	0.157
Extruded alloy	0.378	0.273

3.3 Corrosion morphologies

After the specimens were immersed in 5% NaCl aqueous solution for a certain time, corrosion pits presented on the surface of the specimens. Few of hydrogen bubbles gradually presented on the surface of the Mg−5Y−7Gd−1Nd−0.5Zr alloys at the initial stage, then the number of hydrogen bubbles got to accelerate rapidly. Figure 4 shows the corrosion morphologies of the Mg−5Y−7Gd−1Nd−0.5Zr specimen surfaces immersed in the 5% NaCl aqueous solution for 2 h (as-casting) and 24 h (extrusion) where the corrosion products had been removed. Corrosion initiated from a few small pits and enlarged gradually and new pits occurred subsequently. The α phase which is adjacent with the RE-containing phase was preferentially corroded. Figure 4 shows the magnified assigned morphology of Fig. 4(a), and Fig. 4(f) shows the magnified assigned morphology of Fig. 4(d). Filiform corrosion morphologies are also observed after immersion as shown in Fig. 4, but the degree of filiform corrosion for as-cast Mg−5Y−7Gd−1Nd−0.5Zr alloy is slight. However, the extruded Mg−5Y−7Gd−1Nd−0.5Zr alloy after immersion 24 h does not come up the filiform

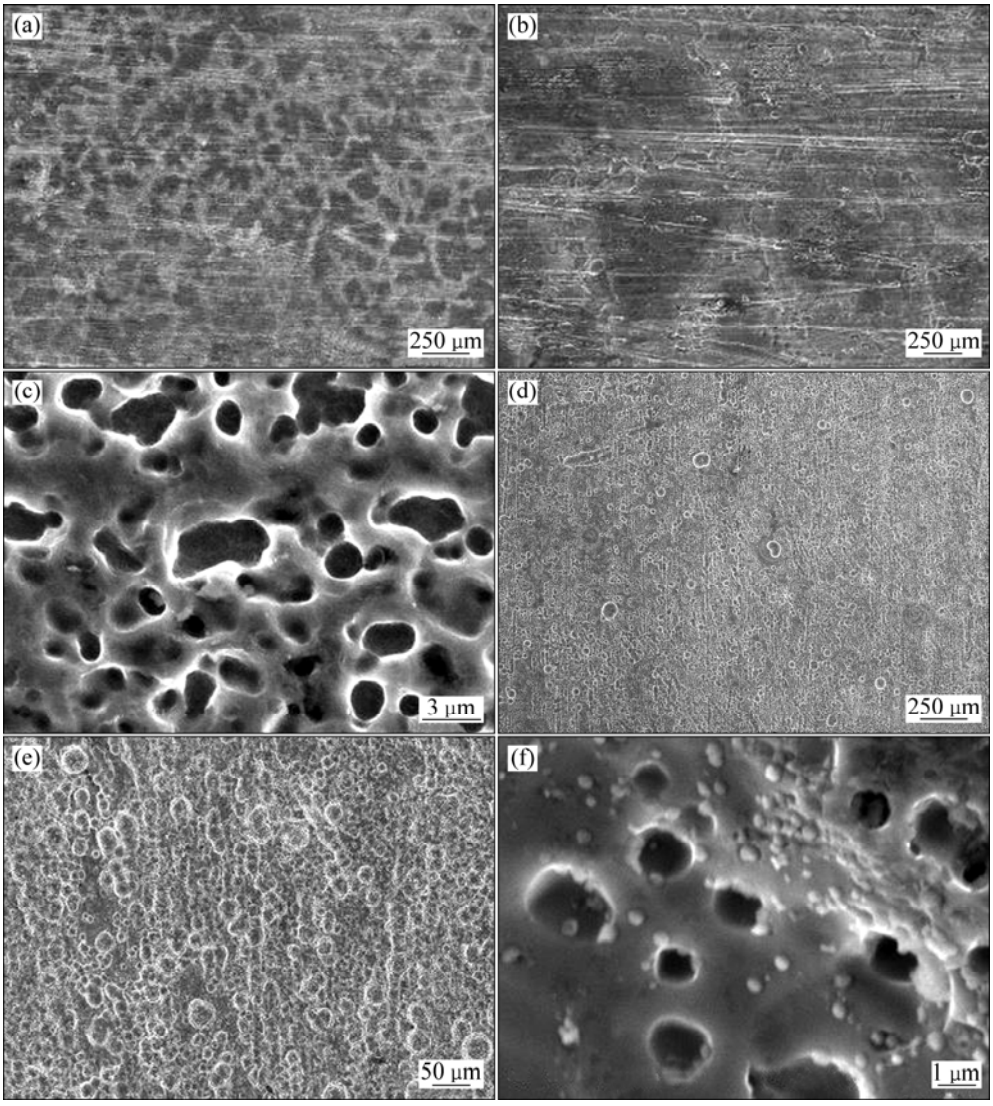

Fig. 4 Surface features of Mg−5Y−7Gd−1Nd−0.5Zr specimens after removing corrosion products by explosion to 5% NaC1 aqueous solution for 2 h (as-casting) (a, b, c) and 24 h (extrusion) (d, e, f)

corrosion because of the grain-refinement. The pitting corrosion for extruded sample turns up later and lighter than that of as-cast sample. Figures 4(c) and (f) show that the mean diameter for pitting corrosion of as-cast sample is double of extruded Mg−5Y−7Gd−1Nd−0.5Zr alloy sample.

There is a white netted phase around almost every dent, as shown Figs. 4(c) and 4(f). An EDS analysis for this phase indicates that the percentage of RE is higher than that in the dent, which means the white phase is the Mg−RE and the dent is likely the primary α-Mg phase. The reason for the formation of the dents is that the corrosion resistance of the α-Mg phase was worse than that of the hypoeutectic Mg−RE phases, so that the α-Mg phase dissolved sooner than the eutectics and ultimately left a dent. There is still some α-Mg phases left on the specimen surface, which implies that the corrosion rate of the specimen immersed in the NaCl solution was possibly quite slow. When α-Mg phase around the Mg−RE phases was corroded out, the Mg−RE connecting α-Mg phases also fall off. The reduction of the second phases caused the reduction of the cathodic fraction on the surface, and finally led to the reduction of corrosion rate. The thin film formed on the Mg−5Y−7Gd−1Nd−0.5Zr at the initial stage of immersion did not show excellent protection to the alloy.

There are some second phases embedded in the wall of corrosion pits in Fig. 5. They play an important role in decelerating the corrosion of α-Mg matrix with the increase of exposure time. Thus, the second phases would act as long-term cathodic phases to decelerate the corrosion of Mg−5Y−7Gd−1Nd−0.5Zr alloy. It is found that the α-Mg matrix surrounding the second phase was depleted due to corrosion, but the second phase still kept intact and protruded from the matrix surface. This result proved that the second phases acted as strong cathodes and the α-Mg matrix surrounding the second phases acted as anode during the corrosion process. The corrosion behavior of Mg−RE−Zr alloys depended on the second phase distribution (continuous or not continuous). In the studied alloys, we recognized any evidence of the second phase acting as the cathodes to decelerate the corrosion rate. In the same time, the corrosion behavior of extruded sample also depended on microstructure and grain size. The corrosion resistance of extruded sample was decreased due to smaller grain size in comparison with the as-cast Mg−5Y−7Gd−1Nd−0.5Zr.

Figure 6 shows the surface features of the as-cast and extruded Mg−5Y−7Gd−1Nd−0.5Zr specimens after removing the corrosion products, which were exposed to 5% NaCl aqueous solution for 24 h, 60 h and 108 h. With the increase of time, the distributions and sizes for the dents on the two specimen surfaces got further

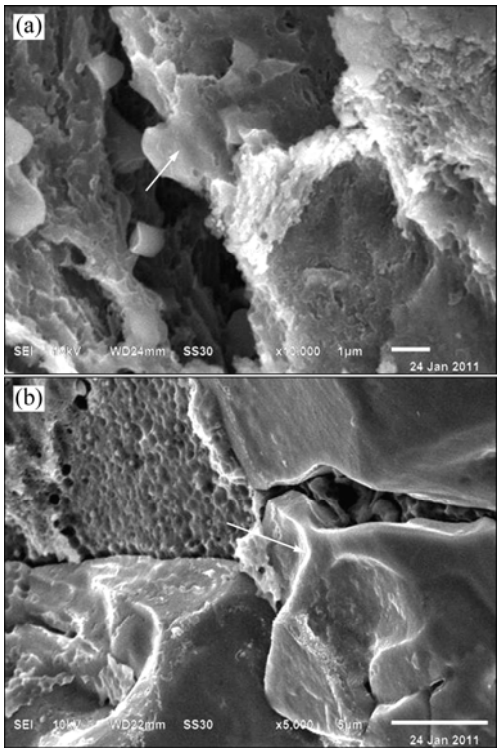

Fig. 5 SEM images of Mg−5Y−7Gd−1Nd−0.5Zr specimens, after removing corrosion products: (a) Extruded specimen; (b) As-cast specimen

aggravated. Comparing the as-cast with the extruded Mg−5Y−7Gd−1Nd−0.5Zr alloys, the dents on the surface of the as-cast sample immersed in the solution appeared much deeper with the increase of exposure time than that of extruded specimen. The corroded surface area of the extruded specimen exhibited corrosion morphology which was aligned in the extrusion direction. The corrosion morphologies of Mg−5Y−7Gd−1Nd−0.5Zr alloy with various exposure time prove that the second phases played an important role in decelerating the corrosion of α-Mg matrix. When Mg−5Y−7Gd−1Nd−0.5Zr alloy was immersed in NaCl solution for 108 h, the corrosion attacks got further aggravated. The surface was covered with a large number of corrosion filaments, resulting in the tracks of corrosion filaments difficult to be identified and the corrosion pits continued to grow in depth direction. These observations again indicated that the corrosion resistance of Mg−5Y−7Gd−1Nd−0.5Zr alloy deteriorated further with increasing the immersion time.

The EDS spectra of Mg−5Y−7Gd−1Nd−0.5Zr alloys after removing the corrosion products are shown in Fig. 7 and Fig. 8. The chemical compositions of the sample surface are shown in the Tables 3 and 4, which show that the as-cast and extruded Mg−5Y−7Gd−1Nd−0.5Zr alloys have the same quantitative chemistry compositions after removing the

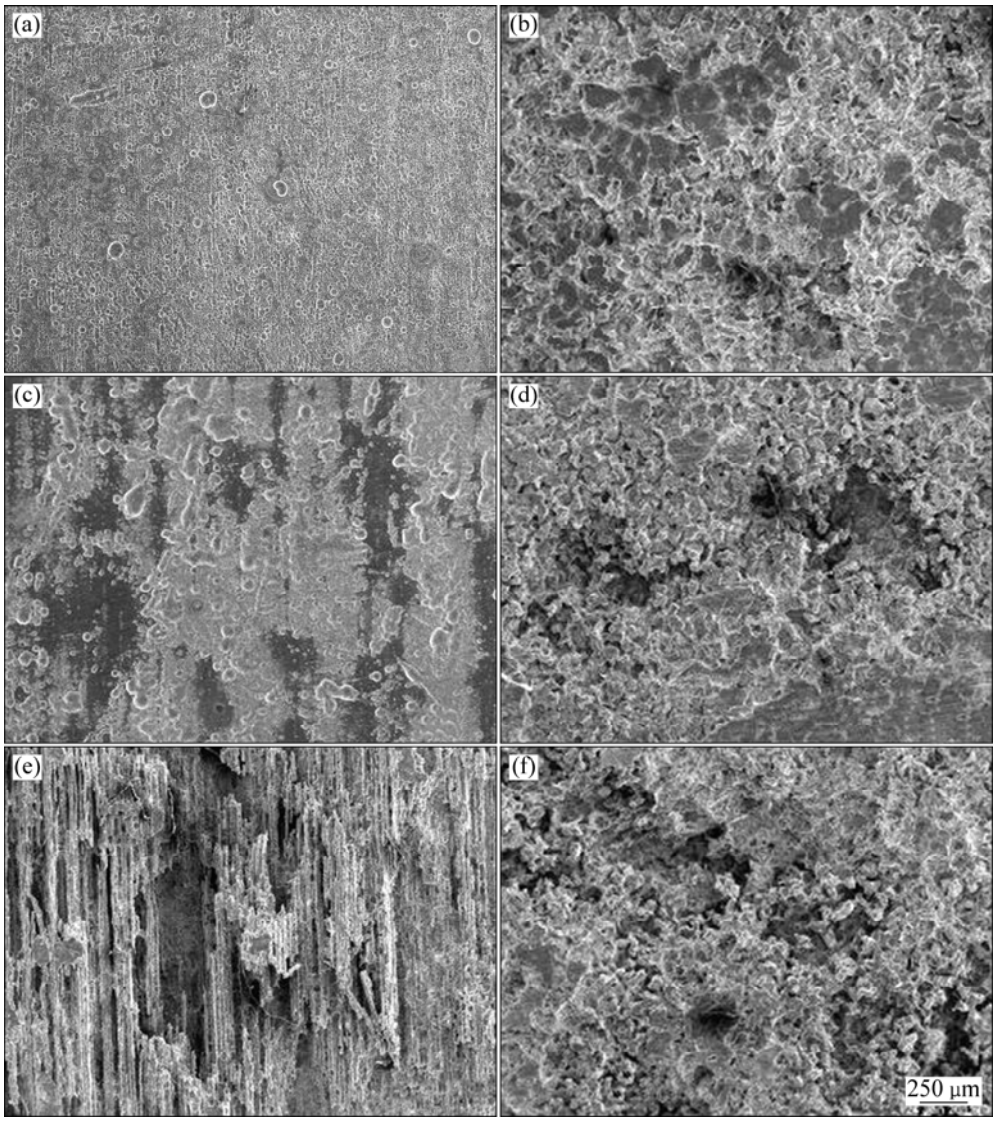

Fig. 6 SEM morphologies of specimens after removing corrosion products formed on specimen surfaces with 24 h (a, b), 60 h (c, d), 108 h (e, f) immersion in 5% NaC1 aqueous solution

corrosion products. The results of chemical composition also indicate that the noble second phase particles are mainly compounds of (Mg, Y, Gd, Nd).

3.4 Open circuit potential

The open circuit potential (φ_{OCP}) experiments were carried out in 5% NaCl solution with saturated $Mg(OH)_2$ and the results are shown in Fig. 9, which disclosed the variation of electrode potential with immersion time. Two principle regularities could be gotten from those curves. First, the curve of Mg−5Y−7Gd−1Nd−0.5Zr sample could be divided into two stages. The corrosion potential of Mg−5Y−7Gd−1Nd−0.5Zr fell down to the lowest one quickly in the initial several seconds as soon as they were immersed into the solution, then fell up quickly. After reaching the low value, the curve of the Mg−5Y−7Gd−1Nd−0.5Zr sample got up slightly with little fluctuation. The value of the open circuit potential kept rapidly moving up and down at −1.658 V and −1.591 V, respectively, during the period of immersion time after 20 min. Some pits were formed and hydrogen bubbles were evolved from the pits. Second, during the exposure time, pure Mg with corrosion potential of −1.790 V [23] showed a more negative corrosion potential than Mg−5Y−7Gd−1Nd−0.5Zr. BIRBILIS et al [24] also found that the corrosion potentials of Mg–RE alloys (Mg–Gd, Mg–Dy, Mg–Nd–Zr, Mg–Gd–Nd–Zr and Mg–Dy–Nd–Zr) were more negative than pure Mg in 5% NaCl solution saturated with $Mg(OH)_2$. It has been reported that rare earth element rich on the surface modifies the surface film of magnesium alloys [25]. For instance, the pseudo-passivation occurs in rapidly solidified Mg−Y alloys. However, the potential of Mg−5Y−7Gd−1Nd−0.5Zr alloy decreased drastically after 20 min and then fluctuated between −1.648 and −1.661 mV, and stabilized at −1.658 mV finally. This

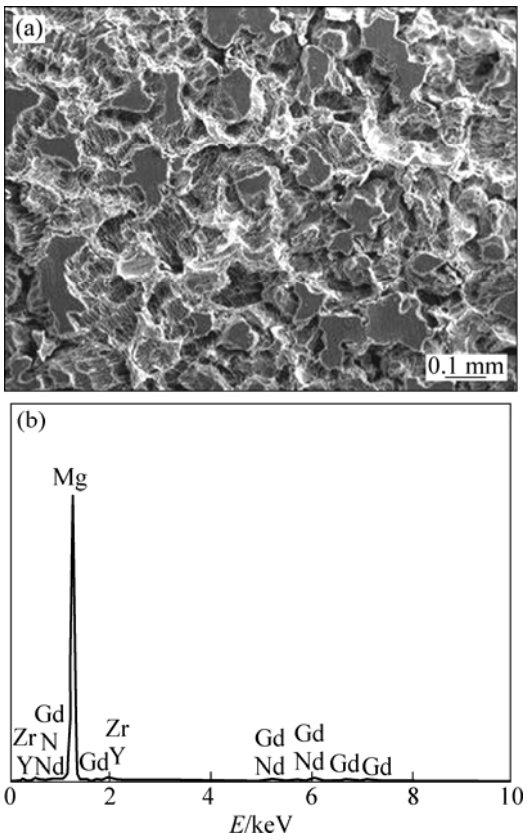

Fig. 7 SEM image (a) and EDS analysis (b) of corroded surface of as-cast Mg−5Y−7Gd−1Nd−0.5Zr alloy

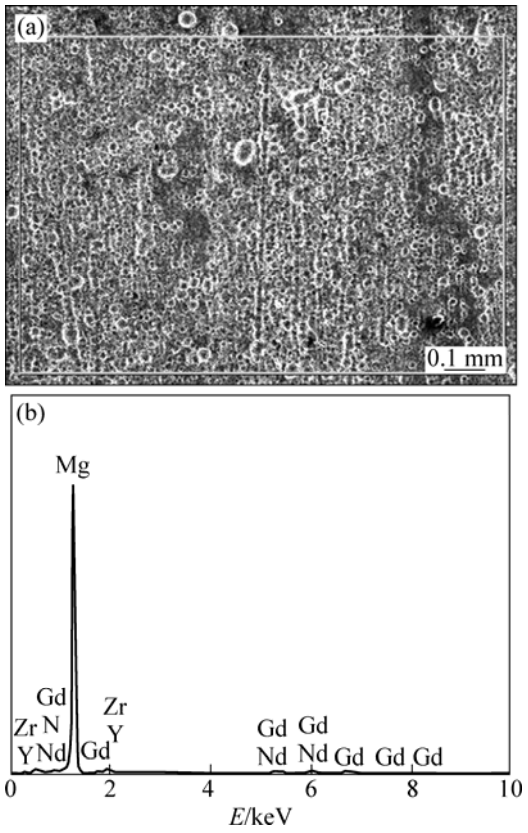

Fig. 8 SEM image (a) and EDS analysis (b) of corroded surface of extruded Mg−5Y−7Gd−1Nd−0.5Zr alloy

Table 3 Quantities for chemical composition of as-cast Mg−5Y−7Gd−1Nd−0.5Zr alloy

Element	*E*/keV	*w*/%	Error/%	*x*/%	*K*/%
Mg	1.253	82.16	0.40	95.83	84.1793
Y	1.922	6.10	2.94	1.63	3.2325
Zr	2.042	1.65	2.56	0.51	1.1303
Nd	5.227	2.18	2.88	0.43	2.4568
Gd	6.053	8.92	3.40	1.60	9.0012
Total		100		100	

Fitting coefficient: 0.3038

Table 4 Quantities for chemical composition of extruded Mg−5Y−7Gd−1Nd−0.5Zr alloy

Element	*E*/keV	*w*/%	Error/%	*x*/%	*K*/%
Mg	1.253	84.55	0.40	96.32	87.6673
Y	1.922	5.74	3.10	1.79	3.4902
Zr	2.042	1.38	2.71	0.42	0.9073
Nd	5.227	0.68	3.07	0.13	0.7230
Gd	6.053	7.65	3.63	1.35	7.3123
Total		100		100	

Fitting coefficient: 0.2986

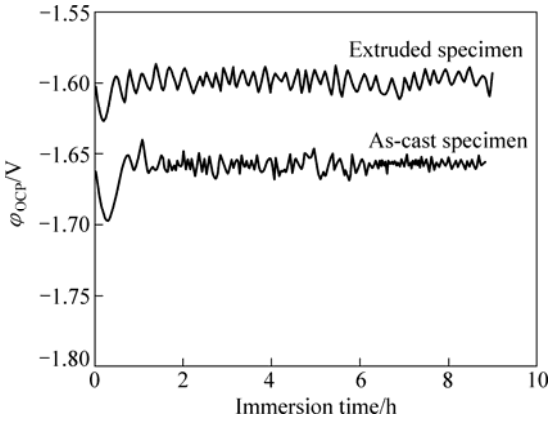

Fig. 9 Variation of open circuit potential of Mg−5Y−7Gd−1Nd−0.5Zr alloy after immersion in 5% NaCl solution saturated by $Mg(OH)_2$ with immersion time

was caused by the fact that magnesium was easily oxidized to form a thick oxide/hydroxide film when it came into contact with humid air or water [26]. The drop in potential after 20 min exhibited that the oxide film reacts quickly with water and forms magnesium hydroxide as follows:

$$MgO+H_2O\rightarrow Mg(OH)_2 \quad (1)$$

After the dissolution of MgO, magnesium substrate would continue to react with the media and magnesium hydroxide is produced and hydrogen gas evolves:

$$Mg+2H_2O\rightarrow Mg(OH)_2+H_2\uparrow \quad (2)$$

Thus, a $Mg(OH)_2$ film would be expected to form on the surface of the Mg−5Y−7Gd−1Nd−0.5Zr alloy. With the development of the reaction, the pH value in the NaCl solution would increase. The Mg^{2+} concentration in the NaCl solution is high, thus OH^- can readily combine with Mg^{2+} to form Mg hydroxide to deposit on the metal surface. This would result in a decrease in OH^- concentration, which would speed up the rate of reaction. The big undulation of Mg−5Y−7Gd−1Nd−0.5Zr in φ_{corr} reflects the formation and breakdown of partially protective film $Mg(OH)_2$.

3.5 Polarization curves

According to the polarization curves, the corrosion current densities J_{corr} of the two specimens in the NaCl aqueous solutions can be obtained by the Tafel extrapolation method. The corrosion potential φ_{corr} values of the as-cast and extruded Mg−5Y−7Gd−1Nd−0.5Zr alloys in the 5% NaCl solutions are −1.658 V and −1.591 V, respectively (in Fig. 10), and the corrosion current density increases with the extrusion.

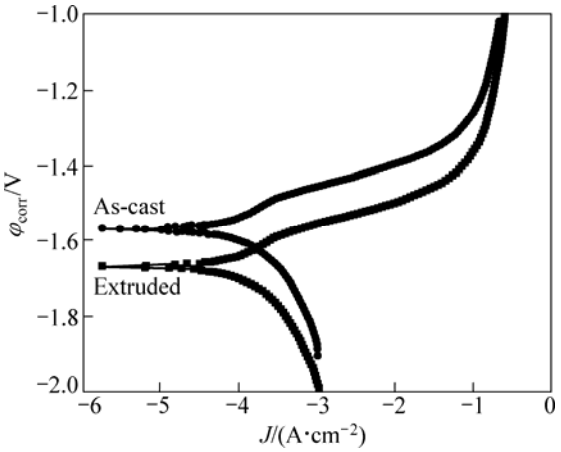

Fig. 10 Polarization curves of as-cast and extruded Mg−5Y−7Gd−1Nd−0.5Zr alloys in 5% NaCl solution

A polarization curve can indicate the tendency of a material to undergo pitting in a specific corrosion environment. The technique is particularly useful in the development of alloys with high pitting resistance [27]. The corrosion result is influenced by the factor of grain size. After the extrusion the grain size decreases due to the fact that the grain size creates more grain boundaries acting as the corrosion barrier.

Generally, the cathodic polarization curves are assumed to represent the cathodic hydrogen evolution, whilst the anodic curves represent the dissolution of magnesium. All specimens reveal an obvious shift of φ_{corr} toward more positive value and a decrease in passive current density with increasing immersion time. It may be due to the nucleation and growth of a thick and semiprotective layer of corrosion products reported by PARDO et al [28]. With increasing the immersion time, the corrosion film got thicker and thicker, the current should go through the corrosion film to get to the sample. The thick corrosion film presents a protective effect of the Mg−5Y−7Gd−1Nd−0.5Zr alloy. The current density increases quickly after the electrode potential exceeding the corrosion potential. This is attributed to the difference between the α-Mg and the second phases and the lower compactness of corrosion product film on Mg−5Y−7Gd−1Nd−0.5Zr alloy. According to the study of HARA et al [29], the corrosion product films formed on Mg alloys during open-circuit immersion were protective and led to spontaneous passivation. When the electrode potential exceeds a critical value (pitting potential), the current density begins to increase sharply. This increase in current density was followed by the evolution of hydrogen on the electrode surface, and the corrosion film suffered local breakdown [27].

Comparing with the pure Mg with φ_{corr} (vs SCE) was −1.790 V, the φ_{corr} values of the as-cast and extruded Mg−5Y−7Gd−1Nd−0.5Zr with different immersion time are higher than −1.658 V, −1.591 V, respectively. NEUBERT et al [30] noted that the corrosion behaviour is one of the critical properties in the application of Mg alloys and can be generally improved by the addition of RE elements. It is shown that the corrosion characteristics of the two alloys studied differ substantially. Although the corrosion resistance of WE43 is not as good as some Mn-containing Mg–RE alloys, it is much better than that of the Mg–Tb–Nd alloy with a similar total concentration of rare earth elements. NAKATSUGAWA et al [31] reported that the addition of heavy rare earth elements is effective in suppressing Mg corrosion. The corrosion rate of the Mg−5Y−7Gd−1Nd−0.5Zr alloy can be slightly reduced by the rare earth.

4 Conclusions

1) Extrusion is a very effective method for grain refinement of Mg−5Y−7Gd−1Nd−0.5Zr alloy. The mean grain sizes of as-cast and extrude alloys are 100 and 15 μm, respectively.

2) The corrosion rate order of the Mg−5Y−7Gd−1Nd−0.5Zr alloys in the 5% NaCl aqueous solutions is as follows: extrusion > as-casting.

3) Extruded and as-cast Mg−5Y−7Gd−1Nd−0.5Zr samples have different corrosion morphologies, but the same chemical composition on the surface after removing the corrosion products.

4) Open circuit potential measurements indicate that the corrosion potential of extruded sample is higher than that of as-cast sample. The polarization values show that extruded sample has higher pitting corrosion resistance than as-cast sample.

Acknowledgements

We gratefully acknowledge the selfless help on alloy electrochemical tests by Dr. MAO Jing-hong, from University of Science and Technology Beijing, China.

References

[1] MAKAR G L, KRUGER J. Corrosion of magnesium [J]. International Materials Reviews, 1993, 38: 138−153.

[2] SONG G, ATRENS A. Corrosion mechanisms of magnesium alloys [J]. Advanced Engineering Materials, 1999, 1: 11−33.

[3] SONG G, ATRENS A. Understanding magnesium corrosion—A framework for improved alloy performance [J]. Advanced Engineering Materials, 2003, 5: 837−858.

[4] SONG G, ATRENS A. Recent insights into the mechanism of magnesium corrosion and research suggestions [J]. Advanced Engineering Materials, 2007, 9: 177−183.

[5] CORRÊA E C S, AGUILAR M T P, SILVA E M, CETLIN P R. The effect of sequential tensile and cyclic torsion straining on work hardening of steel and brass [J]. Journal of Materials Processing Technology, 2003, 142(1): 282−288.

[6] LI L, ZHANG H, ZHOU J, DUSZCZYK J, LI G Y, ZHONG Z H. Numerical and experimental study on the extrusion through a porthole die to produce a hollow magnesium profile with longitudinal weld seams [J]. Materials & Design, 2008, 29(6): 1190−1198.

[7] HAMU G B, ELIEZERA D, WAGNER L. The relation between severe plastic deformation microstructure and corrosion behavior of AZ31 magnesium alloy [J]. Journal of Alloys and Compounds, 2009, 468(1−2): 222−229.

[8] SONG G, ATRENS A, STJOHN D, NAIRN J, LI Y. The electrochemical corrosion of pure magnesium in 1 N NaCl [J]. Corrosion Science, 1997, 39(5): 855−875.

[9] BRUNNER J G, MAY J, HÖPPEL H W, GÖKEN M, VIRTANEN S. Corrosion of ultrafine-grained Al−Mg model alloys [J]. Electrochimica Acta, 2010, 55(6): 1966−1970.

[10] YANG Li-jing, WEI Ying-hua, HOU Li-feng, ZHANG Di. Corrosion behaviour of die-cast AZ91D magnesium alloy in aqueous sulphate solutions [J]. Corrosion Science, 2010, 52(2): 345−351.

[11] BEN-HAROUSH M, BEN-HAMU G, ELIEZER D, WAGNER L. The relation between microstructure and corrosion behavior of AZ80 Mg alloy following different extrusion temperatures [J]. Corrosion Science, 2008, 50(6): 1766−1778.

[12] BEN-HAMU G, ELIEZER D, WAGNER L. The relation between severe plastic deformation microstructure and corrosion behavior of AZ31 magnesium alloy [J]. Journal of Alloys and Compounds, 2009, 468(1−2): 222−229.

[13] LI Y J, ZHANG K, LI X G, MA M L. Evolution of microstructure and mechanical properties of Mg−5Y−5Gd−*x*Nd−0.5Zr magnesium alloys at different states [J]. Rare Metals, 2010, 29(3): 317−322.

[14] BEN-HAMU G, ELIEZER D, SHIN K S, COHEN S. The relation between microstructure and corrosion behavior of Mg–Y–RE–Zr alloys [J]. Journal of Alloys and Compounds, 2007, 431(1−2): 269−276.

[15] ZHANG Xin, ZHANG Kui, LI Xing-gang, WANG Cong, LI Hong-wei, WANG Chang-shun, DENG Xia. Corrosion and electrochemical behavior of as-cast Mg−5Y−7Gd−1Nd−0.5Zr magnesium alloys in 5wt.% NaCl aqueous solution [J]. Progress in Natural Science: Materials International, 2011, 21(4): 314−321.

[16] LI Zhuo-qun, SHAN Da-yong, CHEN Rong-shi, KE Wei, HAN En-hou. Corrosion behavior of W E54 magnesium alloy in 3.5% NaC1 solution [J]. Transactions of Nonferrous Metals Society of China, 2006, 16: 1806−1809.

[17] QUACH N C, UGGOWITZER P J, SCHMUTZ P. Corrosion behaviour of an Mg–Y–RE alloy used in biomedical applications studied by electrochemical techniques [J]. Comptes Rendus Chimie, 2008, 11(9): 1043−1054.

[18] ZHANG Tao, MENG Guo-zhe, SHAO Ya-wei, CUI Zhong-yu, WANG Fu-hui. Corrosion of hot extrusion AZ91 magnesium alloy. Part II: Effect of rare earth element neodymium (Nd) on the corrosion behavior of extruded alloy [J]. Corrosion Science, 2011, 53(9): 2934−2942.

[19] POORQASEMI E, ABOOTALEBI O, PEIKARI M, HAQDAR F. Investigating accuracy of the Tafel extrapolation method in HCl solutions [J]. Corrosion Science, 2009, 51: 1043–1054.

[20] INOUE H, SUGAHARA K, YAMAMOTO A, TSUBAKINO H. Corrosion rate of magnesium and its alloys in buffered chloride solutions [J]. Corrosion Science, 2002, 44(3): 603−610.

[21] ZHANG Tao, SHAO Ya-wei, MENG Guo-zhe, CUI Zhong-yu, WANG Fu-hui. Corrosion of hot extrusion AZ91 magnesium alloy: I-Relation between the microstructure and corrosion behavior, Corrosion Science, 2011, 53(5): 1960−1968.

[22] SONG Dan, MA Ai-bin, JIANG Jing-hua, LIN Ping-hua, YANG Dong-hui, FAN Jun-feng. Corrosion behavior of equal-channel-angular-pressed pure magnesium in NaCl aqueous solution [J]. Corrosion Science, 2010, 52(2): 481−490.

[23] SONG Y W, SHAN D Y, CHEN R S, HAN E H. Corrosion characterization of Mg–8Li alloy in NaCl solution [J]. Corrosion Science, 2009, 51(5): 1087−1094.

[24] BIRBILIS N, CAVANAUGH M K, SUDHOLZ A D, ZHU S M, EASTON M A, GIBSON M A. A combined neural network and mechanistic approach for the prediction of corrosion rate and yield strength of magnesium-rare earth alloys [J]. Corrosion Science, 2011, 53(1): 168−176.

[25] YAMASAKI M, HAYASHI N, IZUMI S, KAWAMUR A Y. Corrosion behavior of rapidly solidified Mg−Zn-rare earth element alloys in NaCl solution [J]. Corrosion Science, 2007, 49: 255−262.

[26] HARA N, KOBAYASHI Y, KAGAYA D, AKAO N. Formation and breakdown of surface films on magnesium and its alloys in aqueous solutions [J]. Corrosion Science, 2007, 49: 166−175.

[27] CHANG J W, PENG L M, GUO X W, ATRENS A, FU P H, DING W J, WANG X S. Comparison of the corrosion behavior in 5wt.% NaCl solution of Mg alloys NZ30K and AZ91D [J]. Journal of Applied Electrochemistry, 2008, 38: 207−214.

[28] PARDO A, MERINO M C, COY A E, ARRABAL R, VIEJO F, MATYKINA E. Corrosion behaviour of magnesium/aluminium alloys in 3.5 wt.% NaCl [J]. Corrosion Science, 2008, 50(3): 823−834.

[29] NOBUYOSHI H, YASUHIRO K, DAISUKE K NOBORU A. Formation and breakdown of surface films on magnesium and its alloys in aqueous solutions [J]. Corrosion Science, 2007, 49(1): 166−175.

[30] NEUBERT V, STULÍKOVÁ I, SMOLA B, MORDIKE B L, VLACH M, BAKKAR A, PELCOVÁ J. Thermal stability and corrosion behaviour of Mg–Y–Nd and Mg–Tb–Nd alloys [J]. Materials Science and Engineering A, 2007, 462(1−2): 329−333.

[31] NAKTSUGAWA I, TAKAYASU H, ARAKI K, TSUKEDA T. Electrochemical corrosion studies of thixomolded AZ9lD in sodium chloride solution [J]. Materials Science Forum, 2003, 419: 845−850.

铸态与挤压态 Mg−5Y−7Gd−1Nd−0.5Zr 合金在 5% NaCl 水溶液中的腐蚀行为

张 新[1,2,3]，张 奎[1]，李兴刚[1]，邓 霞[1]，李宏伟[2,3]，张宝东[2,3]，王长顺[2,3]

1. 北京有色金属研究总院 有色金属材料制备加工国家重点实验室，北京 100088；
2. 北京北方车辆集团有限公司 工艺研究所，北京 100072；
3. 北京市特种车辆部件先进制造与评估工程技术研究中心，北京 100072

摘 要：在 5% NaCl 水溶液中通过浸泡和电化学测试研究铸态与挤压态 Mg−5Y−7Gd−1Nd−0.5Zr 镁合金的腐蚀性能。铸态和挤压态 Mg−5Y−7Gd−1Nd−0.5Zr 镁合金的平均晶粒尺寸分别为 100 μm 和 15 μm。在腐蚀初期，铸态合金的腐蚀形貌为点蚀和少量丝状腐蚀，挤压态合金的腐蚀形貌为点蚀。挤压态合金的腐蚀速率大于铸态合金的腐蚀速率。包含稀土的第二相在合金中作为阴极，改善了合金的腐蚀性能。铸态与挤压态合金的腐蚀电位分别为−1.658 V 和−1.591 V。探讨了铸态与挤压态合金腐蚀性能不同的原因。

关键词：Mg−5Y−7Gd−1Nd−0.5Zr 镁合金；腐蚀形貌；极化曲线

(Edited by YANG Hua)